J|A|C|S COMMUNICATIONS

Published on Web 07/06/2009

Conjugation of Colloidal Clusters and Chains by Capillary Condensation

Fan Li and Andreas Stein*

Department of Chemistry, University of Minnesota, 207 Pleasant Street SE, Minneapolis, Minnesota 55455

Received June 5, 2009; E-mail: a-stein@umn.edu

Colloidal particles featuring anisotropic shapes and functionalities are highly interesting building blocks suitable for self-assembly of complex nanostructured systems.[1] While in certain cases anisotropic particles can be attained by direct syntheses, unique shapes and symmetries can also be achieved by grouping simple particles, such as spherical colloids, into clusters.[2] The pristine clusters, though often referred to as "colloidal molecules",[3] still lack the directional bonding capabilities of their counterparts in the molecular realm. Recently, much effort has been devoted to cluster development and functionalization, including mass production of monodisperse clusters,[4] assembly of hybrid clusters comprising different colloids,[4a,5] preparation of composite clusters decorated with secondary components,[6] etc. Such approaches represent early steps toward mimicking molecular assembly at the colloidal scale and toward the realization of rational colloid assembly processes by true designer pathways.[7]

Herein we describe the application of capillary condensation to modulate colloid connectivity and surface topology, leading to conjugated clusters and chains with anisotropic functionality. Capillary condensation—the phenomenon involving selective condensation of vapor below its saturation vapor pressure in cavities or between surfaces—has been widely employed to modify porous materials[8] and, recently, to adjust the mechanical properties[9] and refractive indices[10] of thin nanoparticle films. Here it is used as an effective means for selective deposition of material that links colloidal nanostructures, as schematically illustrated in Figure 1a. Colloidal chains and colloidal clusters with various aggregation numbers (n) were formed by spin-coating dilute dispersions of polystyrene (PS) spheres in a 50/50 wt % mixture of ethanol and ethylene glycol on a tungsten-coated substrate. The rapid evaporation of ethanol led to formation of sphere domains on the substrate, and the slow removal of ethylene glycol resulted in colloids grouped into close-packed clusters in most areas and a few chains in some locations.[11] When air containing dichloromethylvinylsilane (DCMVS) vapor was passed over the sample, capillary condensation commenced in the vicinity of the contacting points between colloids, and the condensation region gradually expanded to fill the void space until equilibrium was reached. Meanwhile, the highly reactive Si−Cl bonds were hydrolyzed by moisture and through "chemical condensation" converted the condensate into a solid organosilicate. A series of 2D composite clusters and a 1D-connected colloid chain are shown in Figure 1. Previously such composite clusters were synthesized through coassembly of "backbone" colloids and secondary materials, such as nanoparticles[6b] or liquid precursors.[6a,d] The spatial selectivity of capillary condensation is evident from the observation that the templated organosilicate phases (bright bands) reside predominantly between adjacent spheres, different from previous reports, where coassembly led to uniform silicate coatings on the clusters.[6a,12]

The cross-sectional profile of the meniscus at equilibrium was derived as a function of the condensate contact angle and the sphere radius (see the Supporting Information and Figure S2). Since both

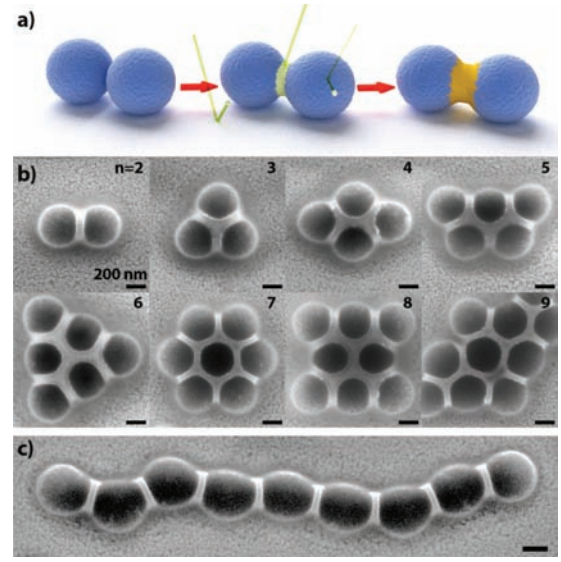

Figure 1. (a) Illustration of the vapor-phase templating process. Vapor condenses preferentially in the intercolloid spaces. (b) SEM micrographs of PS/organosilicate composite colloidal clusters with varying number (n = 2−9) of colloidal building blocks. (c) A colloidal chain connected by organosilicate deposits. All the scale bars represent 200 nm.

of these parameters and the interparticle spacing were nearly constant for the colloids used here, the condensation pattern was also spatially very uniform. However, the actual DCVMS deposition process was further complicated by spontaneous adsorption. Previous studies have revealed that, in association with capillary condensation, a precursor monolayer may also be formed on the substrate due to spontaneous adsorption.[13] Monte Carlo simulations confirmed the propensity of DCMVS molecules to pack loosely on the polystyrene surfaces, forming submonolayers to multiple layers a few nanometers thick, depending on the partial vapor pressure (Figure S3). Such adsorption layers are also visible in the SEM images of some of the clusters (Figure S4), although these could be removed by brief washing with isopropyl alcohol (IPA). The spontaneous adsorption influenced the deposition profile by altering the effective contact angle,[13a] and since it was a function of the partial pressure, it was important to distribute the vapor evenly in the condensation process. When DCMVS vapor was passed over the spheres in a flowing atmosphere, the condensates were confined between spheres, consistent with the calculated equilibrium meniscus in Figure S2b. In a static atmosphere, however, a fraction of clusters closest to the source of DCMVS was coated more extensively with an organosilicate deposit (Figure S4). Note that the precursor vapor could also condense at the colloid−substrate interface. In practice, we found that washing the sample with IPA could efficiently remove the substrate adhesion layer, whereas the deposit between spheres was hardly affected. This may be explained

10.1021/ja904591a CCC: $40.75

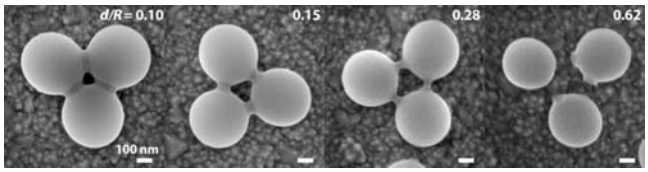

Figure 2. Capillary condensation on nonclose-packed colloidal clusters. The clusters were created by plasma etching of close-packed PS clusters for different times to reach a desired sphere radius (R) and intersphere distance (d, edge-to-edge). The values of d/R are given as a measure of relative intersphere spacing. All the scale bars represent 100 nm.

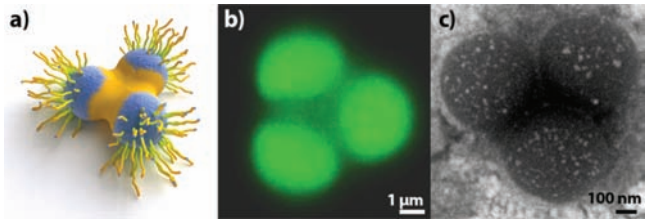

Figure 3. (a) Schematic illustration of a triangle cluster modulated by capillary condensation to create anisotropic functionality. (b) Confocal microscopy image of a fluorescent PS cluster after DCMVS condensation. The weakened fluorescence was caused by the DCMVS deposit. (c) Backscattered SEM image showing the site-specific distribution of Au nanoparticles (white spots) on an amine-functionalized PS cluster.

by the tendency for IPA to slightly lift up the colloidal clusters and thereby remove the condensed material underneath (Figure S5).[14]

Capillary condensation does not require spheres to be in contact. We created different intersphere spacings (d) by oxygen plasma etching the colloids and studied the dependence of the condensation process on the spacing. As shown in Figure 2, the conjugation was well preserved up to the ratio $d/R = 0.28$ (R: colloid radius). Even at $d/R = 0.62$, intersphere capillary condensation still occurred as evidenced by the residue of a precursor bridge, which had, however, been destroyed by capillary forces.[15] Capillary forces could also deform the spheres, which is more apparent for linearly arranged colloids (Figure S6). Although further process optimization is necessary to overcome the capillary forces at large interparticle distances, capillary condensation nevertheless opens up exciting applications in arresting scattered colloidal particles[16] into continuous chains and allows modulation of spacing-related properties.[17]

One objective of this research was to modulate the distribution of surface groups through vapor deposition, leading to functionally anisotropic nanosized building blocks (Figure 3a). The effect of selective organosilicate deposition was visually evident by condensation on clusters of 3-μm fluorescent PS beads. The organosilicate deposit clearly resulted in regional diminution of the fluorescence (Figure 3b). A similar observation has been reported for clusters coassembled with fluorescent polymer colloids.[6c] However, to ensure that the remaining surface was really active rather than being covered by an invisible condensate monolayer, we used amine-functionalized polymer beads and, after deposition, examined the surface amino group distribution by probing with Au nanoparticles (~3 nm). The backscattered SEM image (Figure 3c) confirmed that no chemically adsorbed Au nanoparticles resided in DCMVS-deposited regions; meanwhile the surface was fully covered by Au in other areas of the triangle cluster, which confirms that tethered colloidal clusters could be prepared by this facile approach. In addition, it should be noted that in this study we examined polymer beads with different sizes and surface chemistries (e.g., pristine, plasma-modified, and amine-functionalized surfaces), but the deposition selectivity was never compromised.

In summary, through controlled capillary condensation, regional selectivity could be realized in a vapor phase deposition process on colloidal nanostructures. This approach was successfully used in establishing connections in colloidal clusters and 1D colloidal chains and would be easily adaptable to stabilize colloidal clusters prepared by other methods that produce more controllable cluster sizes and shapes.[4] The capillary condensation method is simple and can be applied to a wide range of materials. It has great tolerance for geometric variations and even permits conjugation of spatially separated particles. The selective deposition was also used to modulate the functionality on the colloid surfaces and led to tip-tethered nanosized building blocks, whose assembly via directional interactions will be the subject of future research.

Acknowledgment. This work was financially supported by the National Science Foundation (DMR-0704312). It was carried out in part at the University of Minnesota (UMN) Characterization Facility and the UMN Nanofabrication Center, which receive partial support from the NSF through the MRSEC, ERC, MRI, and NNIN programs, and used computing resources at the UMN Supercomputing Institute. Fluorescence microscopy was performed in the UMN Biomedical Image Processing Lab.

Supporting Information Available: Experimental details, a qualitative description of the meniscus profile, snapshots of the spontaneous adsorption of DCMVS on a PS surface at various degrees of saturation, SEM images of colloidal clusters and colloidal chains after capillary condensation. This material is available free of charge via the Internet at http://pubs.acs.org.

References

(1) Yang, S. M.; Kim, S. H.; Lim, J. M.; Yi, G. R. *J. Mater. Chem.* **2008**, *18*, 2177–2190.
(2) Manoharan, V. N.; Elsesser, M. T.; Pine, D. J. *Science* **2003**, *301*, 483–487.
(3) van Blaaderen, A. *Nature* **2006**, *439*, 545–546.
(4) (a) Yin, Y.; Lu, Y.; Gates, B.; Xia, Y. *J. Am. Chem. Soc.* **2001**, *123*, 8718–8729. (b) Yi, G. R.; Thorsen, T.; Manoharan, V. N.; Hwang, M. J.; Jeon, S. J.; Pine, D. J.; Quake, S. R.; Yang, S. M. *Adv. Mater.* **2003**, *15*, 1300–1304. (c) Korkut, S.; Saville, D. A.; Aksay, I. A. *Langmuir* **2008**, *24*, 12196–12201.
(5) (a) Yin, Y.; Lu, Y.; Xia, Y. *J. Am. Chem. Soc.* **2001**, *123*, 771–772. (b) Kim, J. W.; Larsen, R. J.; Weitz, D. A. *J. Am. Chem. Soc.* **2006**, *128*, 14374–14377. (c) Kim, J. W.; Larsen, R. J.; Weitz, D. A. *Adv. Mater.* **2007**, *19*, 2005–2009. (d) Ohnuma, A.; Cho, E. C.; Camargo, P. H. C.; Au, L.; Ohtani, B.; Xia, Y. *J. Am. Chem. Soc.* **2009**, *131*, 1352–1353. (e) Yu, H. K.; Mao, Z.; Wang, D. *J. Am. Chem. Soc.* **2009**, *131*, 6366–6367.
(6) (a) Yi, G. R.; Manoharan, V. N.; Michel, E.; Elsesser, M. T.; Yang, S. M.; Pine, D. J. *Adv. Mater.* **2004**, *16*, 1204–1208. (b) Cho, Y. S.; Yi, G. R.; Lim, J. M.; Kim, S. H.; Manoharan, V. N.; Pine, D. J.; Yang, S. M. *J. Am. Chem. Soc.* **2005**, *127*, 15968–15975. (c) Kim, S. H.; Yi, G. R.; Kim, K. H.; Yang, S. M. *Langmuir* **2008**, *24*, 2365–2371. (d) Kraft, D. J.; Vlug, W. S.; van Kats, C. M.; van Blaaderen, A.; Imhof, A.; Kegel, W. K. *J. Am. Chem. Soc.* **2009**, *131*, 1182–1186.
(7) Zerrouki, D.; Baudry, J.; Pine, D.; Chaikin, P.; Bibette, J. *Nature* **2008**, *455*, 380–382.
(8) Lu, A. H.; Schueth, F. *Adv. Mater.* **2006**, *18*, 1793–1805.
(9) Kim, S.; Ehrman, S. H. *Langmuir* **2007**, *23*, 2497–2504.
(10) Gemici, Z.; Schwachulla, P. I.; Williamson, E. H.; Rubner, M. F.; Cohen, R. E. *Nano Lett.* **2009**, *9*, 1064–1070.
(11) Mihi, A.; Ocana, M.; Miguez, H. *Adv. Mater.* **2006**, *18*, 2244–2249.
(12) Ibisate, M.; Zou, Z.; Xia, Y. *Adv. Funct. Mater.* **2006**, *16*, 1627–1632.
(13) (a) Dobbs, H. T.; Darbellay, G. A.; Yeomans, J. M. *Europhys. Lett.* **1992**, *18*, 439–444. (b) Kim, S.; Ehrman, S. H. *J. Chem. Phys.* **2007**, *127*, 134702−1–134702/10.
(14) Sun, F.; Cai, W.; Li, Y.; Cao, B.; Lei, Y.; Zhang, L. *Adv. Funct. Mater.* **2004**, *14*, 283–288.
(15) Rabinovich, Y. I.; Esayanur, M. S.; Moudgil, B. M. *Langmuir* **2005**, *21*, 10992–10997.
(16) Huang, J.; Tao, A. R.; Connor, S.; He, R.; Yang, P. *Nano Lett.* **2006**, *6*, 524–529.
(17) Tao, A. R.; Huang, J.; Yang, P. *Acc. Chem. Res.* **2008**, *41*, 1662–1673.

JA904591A